

Oxygen evolution reaction using EC-MS system

EC-MS Application Note #4

last updated 05-10-2022

Introduction

Understanding and improving material performance for oxygen evolution reaction (OER) is paramount for many renewable energy storage and conversion schemes proposed for a sustainable economy [1]. Hydrogen generation using water electrolysis and CO₂ up-conversion through the CO₂ reduction reaction (CO₂RR), provide promising renewable energy conversion options into fuels and valuable chemicals. In both processes, OER occurs as one of the two half-cell reactions, as illustrated for water electrolysis in figures 1a and b.

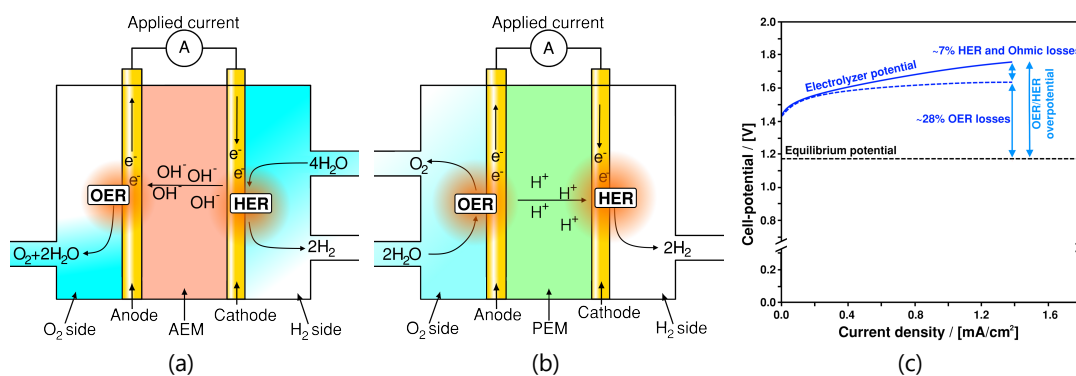


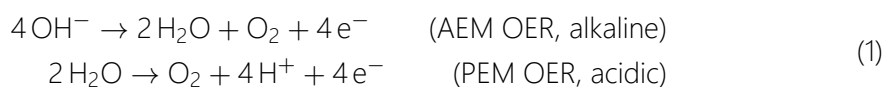
Figure 1: Schematics of (a) AEM electrolyzer operating principle. (b) PEM electrolyzer operating principle. (c) Typical representation of OER overpotential in a PEM electrolyzer stack, adapted from [2]. Note, typical OER overpotential losses in AEM electrolyzers are only ~25% [3] however with significant additional Ohmic and HER associated losses when compared to PEM-based counterparts.

In this application note, we wish to highlight the benefits that can be gained by coupling OER catalyst studies with an EC-MS elucidating this important half-cell reaction. The exact mechanisms through which OER proceeds are still being contested, and can often be considered catalyst dependent. In that context various isotope labeled studies have been suggested in which the catalyst was pre-oxidized with ¹⁸O and then studied using EC-MS [4, 5]. Product detection and complete quantification is enabled by the EC-MS allowing the

true OER activity to be measured - something which may be exceedingly difficult using traditional techniques. In the following, we first provide a brief background to OER research and proceed to showcase the EC-MS capabilities for OER investigation with four simple examples, followed by a brief literature review.

Background

OER can occur both in alkaline and acidic environment and follows the half-cell reactions given in equation 1.



Different electrocatalysts are typically used in alkaline and acidic systems: Inexpensive, stable and abundant OER catalysts typically based on $\text{Ni}_x(\text{Co}_y\text{Fe}_z)$ perform excellent for alkaline OER. They are used in traditional alkaline electrolysis as well as the more recently developed anion exchange membrane (AEM) electrolyzer illustrated in see figure 1. In acidic electrolyzer systems on the other hand, significant issues arise due to material instability at low pH (catalyst oxidation and dissolution). Currently, the only reasonably stable and active OER catalysts for PEM electrolysis are based on IrO_x . However, due to its high price and scarcity, replacing this catalyst is a prerequisite for up-scaling PEM electrolyzers to widespread commercial applications.

Given the present status of alkaline- and acidic polymer electrolyte membrane technologies most OER catalyst studies focus on:

Alkaline OER: Finding nano-materials which constituents (*e.g.* Fe or Co) are unable to crossover to the cathode side disrupting the hydrogen evolution reaction (HER) or ion transport while maintaining high OER activity, *i.e.* low OER overpotential.

Acidic OER: Identifying stable, abundant/inexpensive and electrically conductive materials exhibiting low OER overpotential (see figure 1c) and which elemental constituent do not pose additional crossover issues in terms of membrane and HER deterioration.

Besides studies of materials for these two cases, numerous studies concern the deterioration of support materials both under acidic, neutral and alkaline conditions. For a more in-depth overview to basic OER electrocatalysis we refer readers to the extremely rich OER literature.

Examples of OER studies using the EC-MS

For this document, four catalyst systems were investigated using the EC-MS. They were chosen to: (i) Show consistency with known electrolyte effects for OER [6, 7]. (ii) Showcase the alkaline capabilities of the EC-MS using non-aqueous chips. (iii) Highlight how the EC-MS provides insights that purely electrochemical techniques cannot. These systems are:

- 1-3 Pt_{Poly} (PINE inst., see [8] for proper preparation) in 0.1 M HClO₄, 0.5 M H₂SO₄ or 0.5 M KOH electrolyte, respectively.
- 4 Glassy carbon (GC) (HTW, Sigradur[®] G) in 0.1 M HClO₄ electrolyte.

These systems were tested following the procedure established in *Benchmark Measurements EC-MS Technical Note #2* and prepared by cleaning the EC-MS cell in "Piranha" following *Cleaning Procedures EC-MS Technical Note #12*.

In this section the EC-MS responses recorded while doing cyclic voltammetry (CV) on the samples are discussed. The experimental data is shown in figure 2 and 3, in which signals vs. time and signals vs. potential are presented, respectively.

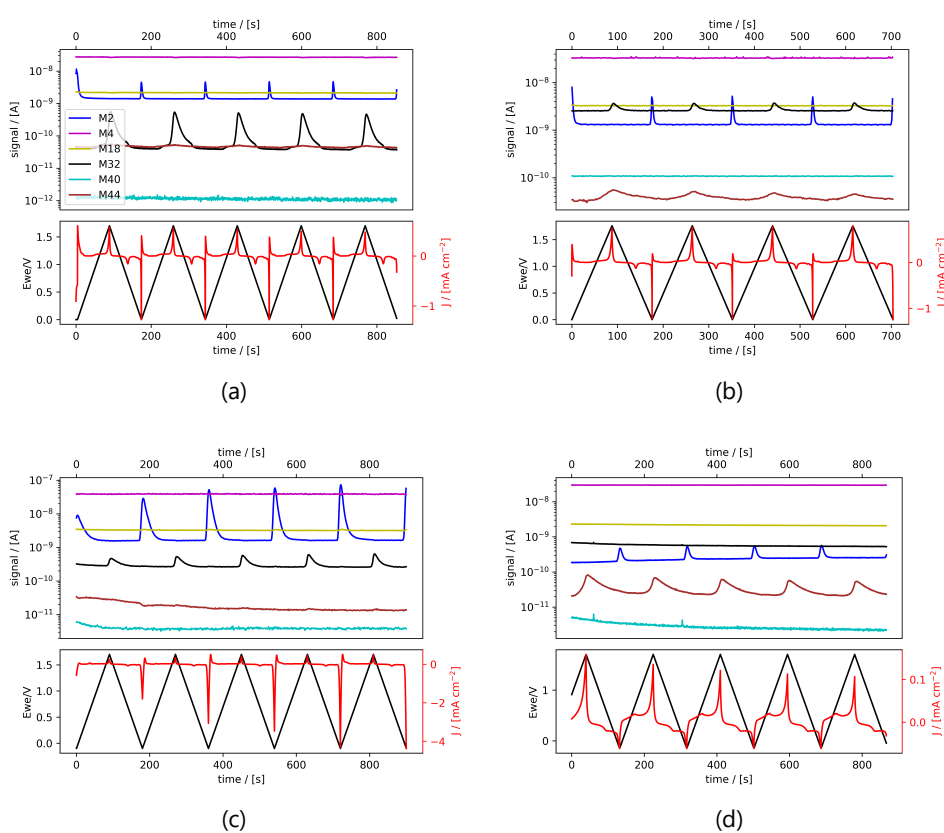


Figure 2: EC-MS plots (room temperature, 20 mV/s, He-saturated, not *IR*-compensated) of (a) Pt_{Poly} in 0.1 M HClO₄. (b) Pt_{Poly} in 0.5 M H₂SO₄. (c) Pt_{Poly} in 0.5 M KOH. (d) GC in 0.1 M HClO₄. Masses correspond to M₂ = H₂, M₄ = He, M₁₈ = H₂O, M₂₈ = N₂/CO, M₃₂ = O₂ and M₄₄ = CO₂.

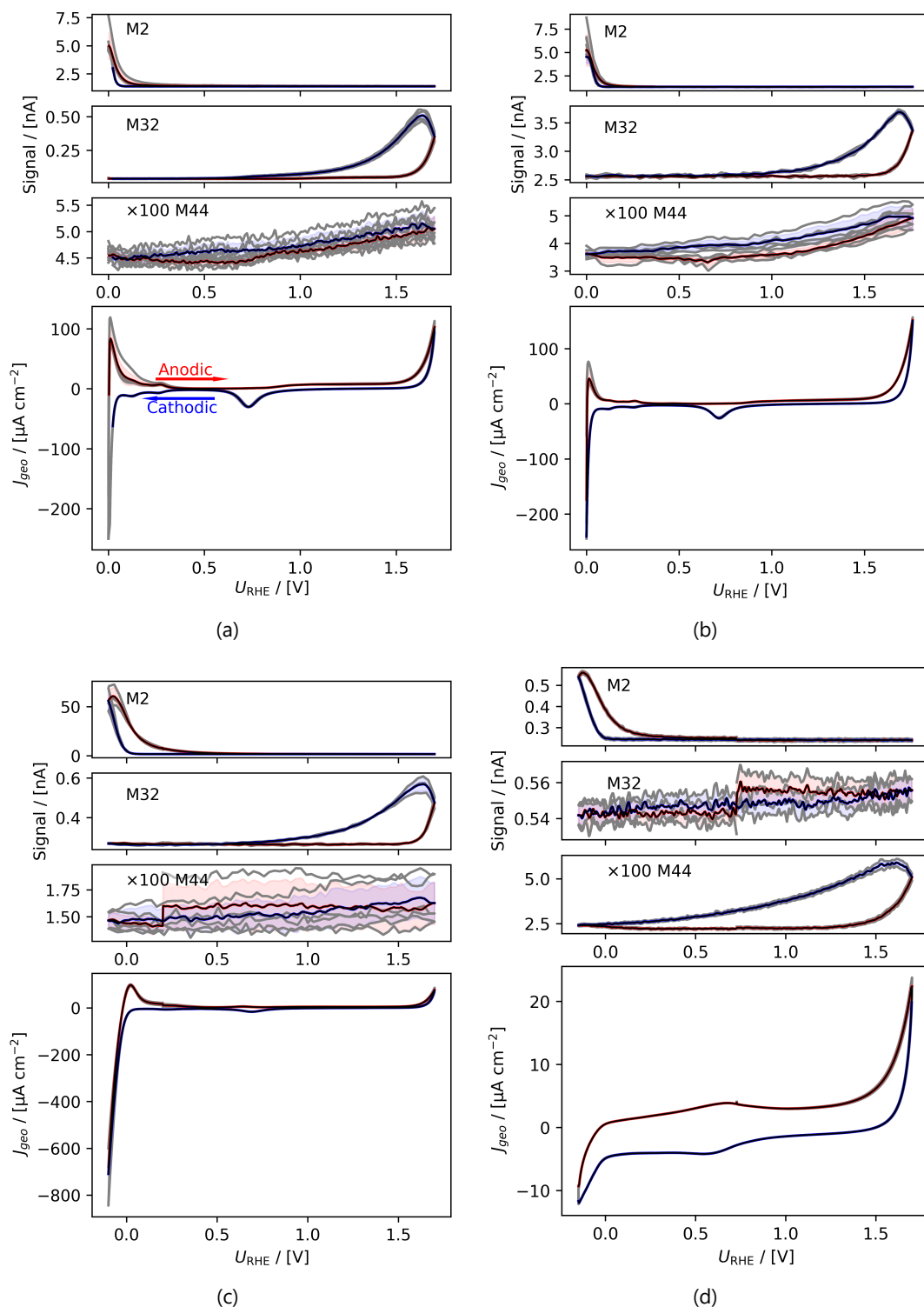


Figure 3: Averaged, IR compensated CVs of EC-MS experiments (from figure 2) co-plotted with $M2 = H_2$, $M32 = O_2$ and $M44 = CO_2$ signals. (a) Pt_{poly} in 0.1 M $HClO_4$. (b) Pt_{poly} in 0.5 M H_2SO_4 . (c) Pt_{poly} in 0.5 M KOH . (d) GC in 0.1 M $HClO_4$. All taken at room temperature and 20 mV/s in He-saturated electrolytes. Note, averaging background noise, as is the instance for the M44 and M32 signal for the Pt_{poly} in KOH and the GC electrode, respectively, results in noisy MS signal curves.

From figure 2 it is noticed that at cathodic (*i.e.* low) potentials significant currents associated with HER (seen as M2 peaks) are observed. Even on the GC electrode hydrogen is formed, albeit at significant lower potentials than on the Pt_{Poly} (in good agreement with work by *Stephens et al.* [9]).

Importantly, figure 2 also highlights significant OER activity on Pt_{Poly} in all three electrolytes, seen as an increase in the M32 signal (associated with O₂), when going to sufficiently anodic (*i.e.* high) potentials. On the GC sample, however, no increase in M32 signal is observed, despite a significant increase in current at anodic potential. At the same time, significant M44 signal increase (associated with CO₂ production) is observed alongside the increase in current. Pt also shows some increase in M44 signal when going to potentials above 0.7V_{RHE}, but to a far lesser extent. To properly capture the potential dependence of the HER-, OER- and CO₂ production onset the results of figure 2 have been averaged using the *Python* package *ixdat*, see figure 3.

Figure 3 again clearly showcases HER and OER for Pt_{Poly} while GC exhibits significant lower propensity towards HER and none towards OER. Rather, GC presents notable CO₂ production. Essentially, going to sufficiently anodic potentials with GC suggest that once O₂ can bind to carbon it is thermodynamic more favourable to form CO₂ rather than O₂. From figure 3 three main conclusions can be drawn:

- 1) In some scientific literature, when researchers utilize carbon-based and/or carbon-supported OER catalysts the observed current above 1.23 eV is often indiscriminately assigned purely to OER. However, the EC-MS data shows direct evidence that this is not the case (CO₂ production on GC). **Thus, to determine true OER current of such catalysts, performing gas analysis is crucial.**
- 2) Pt (and also other non-carbon-based systems) exhibit slight M44 (CO₂) evolution above 0.7V_{RHE}, which arise from trace amounts of carbon impurities of the system. These originate *e.g.* from electrolyte “ageing” and/or adsorption of adventitious adsorbed carbon material introduced from the surrounding ambient environment during assembly/transfers *etc.* The CO₂ signal from the Pt system therefore provides the user with a very good idea of the **degree of carbon contamination of their electrochemical system and/or catalyst material.** Being able to determine contamination directly from the EC-MS data is a huge benefit when testing novel nanocatalysts produced under rather carbon rich conditions.
- 3) Also dissolution of catalyst material can be an issue when determining the faradaic efficiency (FE) towards OER. To evaluate the true FE, two approaches are available: *i)* Quantify dissolution and/or oxidation by other means *e.g.* by using ICP-MS to determine metal concentrations and integrating reduction peaks to estimate the amount of surface oxidation; or *ii)* **Follow the M32 signal using EC-MS, calibrate the system to quantify the O₂ signal and compare the result with the total charge transfer.** This is described in the *EC-MS quantification EC-MS Application Note #2* and the available EC-MS based OER (or OER adjacent) literature [3, 4, 9–17]

OER relevant studies using the EC-MS in literature

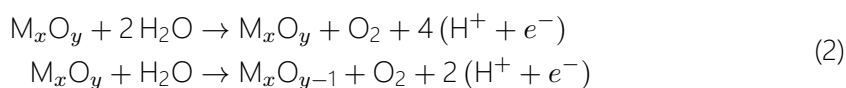
Significant insight on OER can be acquired using Spectro Inlets EC-MS system - insight relevant both for commercial development of OER technologies (electrolyzers, nanomaterial producers etc.) as well as for the scientific electrocatalytic community as a whole. Examples of the unique insights provided by the EC-MS will be presented in the following along with highlighted publications demonstrating specific user cases.

Identification of OER current and specific turn-over frequencies

The most obvious benefit of the EC-MS for investigating OER electrocatalysis is its inherent ability to quantify the O₂ mass signal and subsequently correlate the amount of O₂ evolved to the anodic current. This allows for accurate determination of the true OER onset potential [10, 13, 14] and calculation of turn-over frequencies (TOFs)[4]. At the same time, also other volatile reaction products from parasitic reactions can be detected qualitatively and quantitatively, such as CO₂ from carbon oxidation [10, 12, 16]. Implicitly, this kind of quantitative experiments can also give insights to catalyst stability, for instance when studying IrO_x and RuO_x - two very active OER catalysts in acid. By employing the EC-MS one can, by comparing integrated oxygen charge and current, evaluate to what extent charges for the different catalysts actually produce oxygen or undergo other oxidative processes [10, 13, 14].

Mechanistic OER studies through isotope labeling

Various mechanistic models exist for explaining activity in OER catalysis. An obvious question in this regard is whether the evolved oxygen arises directly from the water or it arises from dissociation of an oxide which is then re-oxidized after the release of O₂. Such complex mechanism can crudely be simplified as indicated here for a metal-oxide (M_xO_y):



While the two pathways of eqn. (2) both produce molecular oxygen as the end product, the pathways are not equivalent. The latter scheme requires an increase in the metal-oxide catalyst oxidation number followed by partial reduction. By selectively pre-oxidizing the M_xO_y catalyst with labeled oxygen (¹⁸O) one can evaluate whether oxygen produced during OER contains mainly M₃₂ or M₃₄ from ¹⁶O₂ or ¹⁶O¹⁸O, respectively. The ratio of produced isotope labeled oxygen can then be compared with non-labeled equivalents to determine whether or not oxygen from the metal oxide participates in the OER mechanism [4, 10] and also gives implicit insights to the stability of oxides for OER.

Insight to support and electrolyte stability

Another extremely important aspect of OER which can be elucidated by the EC-MS concerns the support and the support materials' interaction with the catalyst. For instance,

carbon materials are known to degrade significantly above $1.3V_{\text{RHE}}$. Essentially, carbon degradation occurs as oxidization to CO_2 (M44) which can be directly observed using the EC-MS and has been the topic of several publications [10, 12, 15, 16]. Besides investigating support stability the EC-MS also allows direct evaluation of the electrolyte. In recent years the effects of the electrolyte on OER (e.g. varying anion- and cation concentrations, pH etc.) have been investigated [6, 7]. Some of these electrolytes are not particularly stable under as oxidizing conditions as those needed for OER. Hence, by adding certain components to an electrolyte one may, by just observing the electrochemical current, erroneously count charge transfers arising from electrolyte oxidation and not OER. The EC-MS uniquely gives researchers the possibility to measure O_2 directly and thereby exclude contributions from the electrolyte to the current.

Summary

Here, we have demonstrated how simple OER investigations can be conducted using the EC-MS system and given a brief introduction into mechanistic, isotope, stability and activity aspects relevant for OER.

We showed the M32 signal can be used to determine OER occurrence and how the EC-MS is able to promote direct insights to fundamental reaction phenomena taking place on an electrode surface.

References

- [1] S. Chu, Y. Cui, and N. Liu, "The path towards sustainable energy," *Nature Materials*, vol. 16, no. 1, pp. 16–22, 2016. DOI: [10.1038/nmat4834](https://doi.org/10.1038/nmat4834).
- [2] H. A. Gasteiger, S. S. Kocha, B. Sompalli, and F. T. Wagner, "Activity benchmarks and requirements for Pt, Pt-alloy, and non-Pt oxygen reduction catalysts for PEMFCs," *Applied Catalysis B: Environmental*, vol. 56, no. 1-2, pp. 9–35, 2005. DOI: [10.1016/j.apcatb.2004.06.021](https://doi.org/10.1016/j.apcatb.2004.06.021).
- [3] M. R. Gerhardt *et al.*, "Method—practices and pitfalls in voltage breakdown analysis of electrochemical energy-conversion systems," *Journal of The Electrochemical Society*, vol. 168, no. 7, p. 074503, Jul. 2021. DOI: [10.1149/1945-7111/abf061](https://doi.org/10.1149/1945-7111/abf061).
- [4] C. Roy *et al.*, "Impact of nanoparticle size and lattice oxygen on water oxidation on NiFeOxHy," *Nature Catalysis*, vol. 1, no. 11, pp. 820–829, 2018. DOI: [0.1038/s41929-018-0162-x](https://doi.org/10.1038/s41929-018-0162-x).
- [5] A. Grimaud *et al.*, "Activating lattice oxygen redox reactions in metal oxides to catalyse oxygen evolution," *Nature chemistry*, vol. 9, no. 5, pp. 457–465, 2017. DOI: [10.1038/nchem.2695](https://doi.org/10.1038/nchem.2695).

- [6] A. Ganassin, V. Colic, J. Tymoczko, A. S. Bandarenka, and W. Schuhmann, "Non-covalent interactions in water electrolysis: Influence on the activity of Pt (111) and iridium oxide catalysts in acidic media," *Physical Chemistry Chemical Physics*, vol. 17, no. 13, pp. 8349–8355, 2015. DOI: [10.1039/C4CP04791E](https://doi.org/10.1039/C4CP04791E).
- [7] J. A. Arminio-Ravelo, A. W. Jensen, K. D. Jensen, J. Quinson, and M. Escudero-Escribano, "Electrolyte effects on the electrocatalytic performance of iridium-based nanoparticles for oxygen evolution in rotating disc electrodes," *ChemPhysChem*, vol. 20, no. 22, pp. 2956–2963, 2019. DOI: [10.1002/cphc.201900902](https://doi.org/10.1002/cphc.201900902).
- [8] J. Clavilier, R. Faure, G. Guinet, and R. Durand, "Preparation of monocrystalline Pt microelectrodes and electrochemical study of the plane surfaces cut in the direction of the {111} and {110} planes," *Journal of Electroanalytical Chemistry and Interfacial Electrochemistry*, vol. 107, no. 1, pp. 205–209, 1980, ISSN: 0022-0728. DOI: [10.1016/S0022-0728\(79\)80022-4](https://doi.org/10.1016/S0022-0728(79)80022-4).
- [9] R. P. Oates *et al.*, "How to minimise hydrogen evolution on carbon based materials?" *Journal of The Electrochemical Society*, vol. 169, no. 5, p. 054 516, May 2022. DOI: [10.1149/1945-7111/ac67f7](https://doi.org/10.1149/1945-7111/ac67f7).
- [10] J. Huang, S. B. Scott, I. Chorkendorff, and Z. Wen, "Online electrochemistry–mass spectrometry evaluation of the acidic oxygen evolution reaction at supported catalysts," *ACS Catalysis*, vol. 11, no. 20, pp. 12 745–12 753, 2021. DOI: [10.1021/acscatal.1c03430](https://doi.org/10.1021/acscatal.1c03430).
- [11] K. Kreml *et al.*, "Dynamic interfacial reaction rates from electrochemistry–mass spectrometry," *Analytical Chemistry*, vol. 93, no. 18, pp. 7022–7028, 2021. DOI: [10.1021/acs.analchem.1c00110](https://doi.org/10.1021/acs.analchem.1c00110).
- [12] L. Moriau *et al.*, "Enhancing iridium nanoparticles' oxygen evolution reaction activity and stability by adjusting the coverage of titanium oxynitride flakes on reduced graphene oxide nanoribbons' support," *Advanced Materials Interfaces*, vol. 8, no. 17, p. 2 100 900, 2021. DOI: [10.1002/admi.202100900](https://doi.org/10.1002/admi.202100900).
- [13] S. B. Scott *et al.*, "The low overpotential regime of acidic water oxidation part I: The importance of O₂ detection," *Energy & Environmental Science*, vol. 15, no. 5, pp. 1977–1987, 2022. DOI: [10.1039/D1EE03914H](https://doi.org/10.1039/D1EE03914H).
- [14] S. B. Scott *et al.*, "The low overpotential regime of acidic water oxidation part II: Trends in metal and oxygen stability numbers," *Energy & Environmental Science*, vol. 15, no. 5, pp. 1988–2001, 2022. DOI: [10.1039/D1EE03915F](https://doi.org/10.1039/D1EE03915F).
- [15] S. B. Scott, J. Kibsgaard, P. C. Vesborg, and I. Chorkendorff, "Tracking oxygen atoms in electrochemical CO oxidation–part i: Oxygen exchange via CO₂ hydration," *Electrochimica Acta*, vol. 374, p. 137 842, 2021. DOI: [10.1016/j.electacta.2021.137842](https://doi.org/10.1016/j.electacta.2021.137842).
- [16] M. Smiljanić *et al.*, "Electrochemical stability and degradation mechanisms of commercial carbon-supported gold nanoparticles in acidic media," *The Journal of Physical Chemistry C*, vol. 125, no. 1, pp. 635–647, 2021. DOI: [10.1021/acs.jpcc.0c10033](https://doi.org/10.1021/acs.jpcc.0c10033).

- [17] C. Stumm *et al.*, "Model electrocatalysts for the oxidation of rechargeable electrofuels-carbon supported Pt nanoparticles prepared in UHV," *Electrochimica Acta*, vol. 389, p. 138 716, 2021. DOI: [10.1016/j.electacta.2021.138716](https://doi.org/10.1016/j.electacta.2021.138716).

All data treatment and plotting in this application note was carried out using the open source *Python* package *ixdat*, available at <https://github.com/ixdat/ixdat>.